

## X-ray and Neutron Investigations of the $P\bar{1}-I\bar{1}$ Transition in Anorthite with Low Albite Content

BY W. ADLHART, F. FREY AND H. JAGODZINSKI

*Institut für Kristallographie und Mineralogie der Universität München, Theresienstrasse 41, 8000 München 2, Federal Republic of Germany*

(Received 10 July 1979; accepted 14 November 1979)

### Abstract

Three different samples with an albite concentration of 2.5% and one with an albite concentration of 4.5% were used to investigate the behaviour of  $c$  and  $d$  reflections in a temperature range of 143 to 570 K by X-rays and neutrons. As for  $An_{100}$  the phase transition  $P\bar{1}-I\bar{1}$  is complete and reversible, but in contrast to  $An_{100}$  a definite transition point cannot be determined. Furthermore, the temperature range of the phase transition is shifted to lower temperatures. With increasing albite concentration the characteristics of a well-defined phase transition disappear. The temperature dependence of the  $c$  and  $d$  intensities and the anisotropy of the diffuse scattering contributions are similar to those of  $An_{100}$ ; therefore, they are traced back to the same dynamical origin. The additional influence of antiphase domain boundaries on the line profiles of the  $c$  and  $d$  reflections is discussed.

### I. Introduction

The phase transition  $P\bar{1}-I\bar{1}$  of pure anorthite was the subject of a preceding publication (Adlhart, Frey & Jagodzinski, 1980) which will be referred to as part I throughout this paper. In pure anorthite the sharp  $c$  and  $d$  reflections vanish at  $513 \pm 4$  K. The intensity of these reflections does not only depend heavily on temperature but also on the chemical composition,  $Ca_xNa_{1-x}[Al_{1+x}Si_{3-x}O_8]$ . Moreover, their line profiles are influenced by even a low albite concentration and by the thermal and the mechanical history (Müller, Wenk & Thomas, 1972).

We concentrate our investigation solely on the influence of temperature and chemical composition. The samples used are natural terrestrial plagioclases whose chemical composition and formation are well known from their locality. A clear separation of the effects caused by temperature and those attributed to the chemical composition is only possible for pure  $An_{100}$  ( $x = 1$ ), where it may be assumed that slight

chemical impurities hardly influence the dynamical process. Consequently, the temperature influence can be studied separately (part I).

In this work, samples within a concentration range of  $0.954 \geq x \geq 0.975$  were used. Even these low albite concentrations ( $1 - x$ ) cause much more complex behaviour compared to  $An_{100}$  owing to the simultaneous occurrence of static and dynamic disorder phenomena as well as mutual interactions. So far the diffuse line profiles of the  $c$  and  $d$  reflections have been explained by a strictly static type of disorder, namely antiphase domains (APD) (Laves, Czank & Schulz, 1970; Czank, Van Landuyt, Schulz, Laves & Amelinckx, 1973). In our investigations we discuss only APD's related to the  $I\bar{1}-P\bar{1}$  transition, usually called  $c$  domains in the literature. Their fault vector is  $\frac{1}{2}(\mathbf{a} + \mathbf{b} + \mathbf{c})$  and their domain structure can be studied with  $c$  and  $d$  reflections by electron microscopy (Müller, Wenk & Thomas, 1972; Müller, Wenk, Bell & Thomas, 1973; Czank *et al.*, 1973; McLaren & Marshall, 1974). These studies reveal that the shape of the  $c$  domains is columnar with the largest extension along the  $[2\bar{3}1]$  direction. Their size varies between 70–100 Å for  $An_{95.4}$  (Miyake) (Müller, Wenk & Thomas, 1973), and some  $\mu\text{m}$  for  $An_{97.5}$  (Mt. Somma) (Heuer & Nord, 1976). The varying data for the size of the domains are apparently due to lack of an exact analysis of the anisotropy of the domains. Furthermore, the great influence of the thermal history on the size of the domains is pointed out in the literature. Weak diffuse scattering, showing the same anisotropy as reported for the diffuse  $c$  reflections, may also be observed around the  $a$  reflections in feldspars having a higher Ab content (Jagodzinski & Korekawa, 1973). This scattering might be caused by the  $c$  domain boundaries, but it was not observed for the samples dealt with here.

In addition to the  $c$  domains, the  $b$  domains with a fault vector  $\frac{1}{2}(\mathbf{a} + \mathbf{b})$  may also affect the line profiles of the  $d$  reflections. For our samples we did not observe any difference between the line profiles of the  $b$  and  $a$  reflections and therefore the influence of the  $b$  domains

can obviously be neglected. Therefore we limit our study to the  $c$  domains and their influence on the  $c$  and  $d$  reflections.

To our knowledge, there exist two models to explain the fault vector  $\frac{1}{2}[111]$ . Czank *et al.* (1973) refer to the two subcells in the elementary cell which are displaced by the  $\frac{1}{2}[111]$  vector and only differ by small changes of the atomic positions. An APD boundary occurs when two subcells of the same type are immediate neighbours in the  $[111]$  direction. Since the Si-Al distribution in two cells separated by the antiphase vector is equal from a topological point of view, only small displacements of the atoms are necessary to create this boundary; they may be caused by faults during the nucleation of the  $P\bar{1}$  phase coming from the  $I\bar{1}$  phase. Jagodzinski & Korekawa (1976) suggest that errors in the Si-Al sequence occur when albite molecules are built in the framework at high temperatures. A part of these errors may lead to antiphase domain boundaries with a fault vector  $\frac{1}{2}[111]$ .

X-ray investigations have shown that with rising temperature the intensity of the  $c$  and  $d$  reflections of plagioclases with low albite content decreases rapidly, and simultaneously the line profiles become diffuse (Brown, Hoffman & Laves, 1963; Foit & Peacor, 1973; Laves, Czank & Schulz, 1970). A comparison between the behaviour at the phase transition of crystals with different albite concentrations indicates that both the intensity curve within the transition range and the temperature of transition change drastically. Investigations by electron microscopy reveal that the domain size remains constant when heating the sample.

At temperatures around 470–520 K the contrast of the  $c$  domains disappears but even after heating the sample up to 770 K the original domain structure reappears when the sample is cooled below 470 K (Heuer, Nord, Lally & Christie, 1976). Obviously, a constant domain size and a temperature-dependent reflection width, as observed with X-rays, are contradictory; thus the origin of the diffuse scattering is not clear, especially as the elastic and inelastic contributions have not been separated so far. To our knowledge no publications exist where the observations described above, and their possible connections with the phase transition, are discussed. The aim of this paper is a comprehensive study of the line profiles of the  $c$  and  $d$  reflections as well as the diffuse scattering by X-ray and neutrons. In addition, we tried to find out about the structural changes responsible for the diffuse scattering as a function of temperature and albite concentration.

## II. Results

Crystals from Mt. Somma (An content = 97.5%; Czank *et al.*, 1973) were used for X-ray and neutron measurements and had a mosaic spread of  $<3'$  and  $<10'$ , respectively. Another sample from Minillo (An content = 97.5%) with a similar mosaic spread but with an intergrowth of two grains with a relative tilt angle of about  $15'$  was investigated by neutrons only. Unfortunately, a crystal from Miyake (An content = 95.4%; McLaren & Marshall, 1974) could only be used for X-ray measurements because of its large and

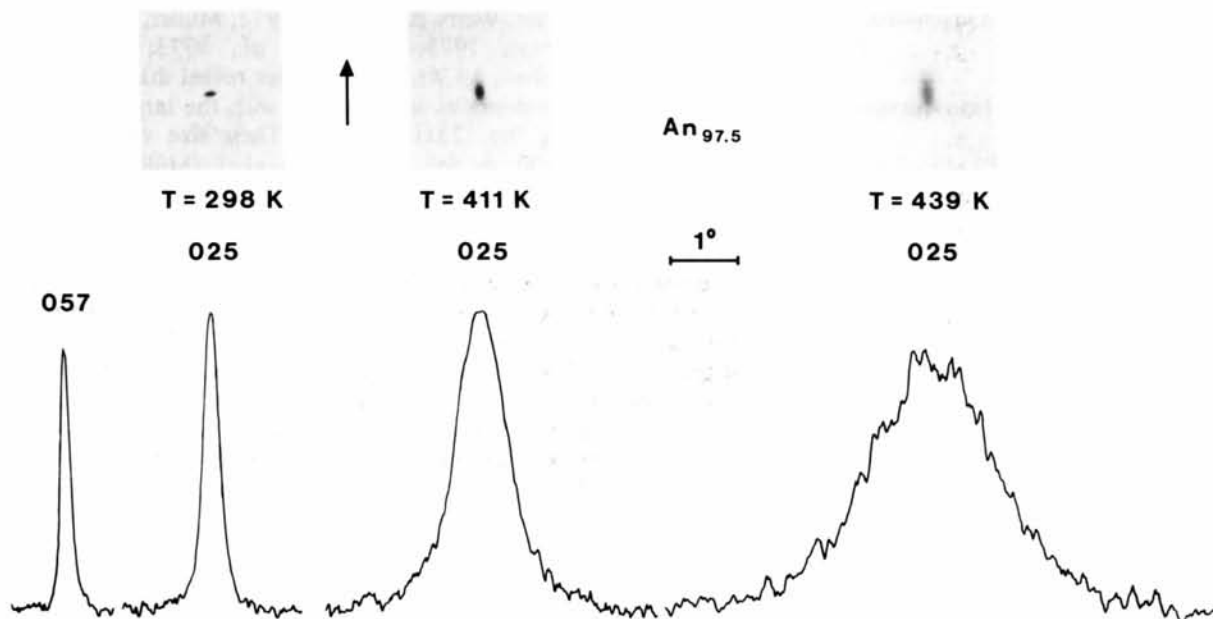


Fig. 1. Magnified area around the 025 reflection from oscillation photographs of  $An_{97.5}$  in a focusing camera. The arrow indicates the direction of the  $a$  axis and the scan direction of the corresponding photometer curves. The resolution of the photograph is shown by the 057 reflection.

inhomogeneous mosaic spread of  $22'$ . For experimental details concerning the measuring techniques see part I.

(a) X-rays

The film and counter measurements were performed with  $\text{Cu } K\alpha_1$  radiation and samples whose  $a$  axis was mounted parallel to the goniometer axis. The photographs were taken with oscillation and Weissenberg techniques. Fig. 1 shows a magnified range around the 025 reflection of oscillation photographs and the corresponding photometer curves at various temperatures. The photometer curves were taken along the focusing direction, *i.e.* perpendicular to the  $\mathbf{b}^*\mathbf{c}^*$  plane.

For all temperatures chosen in our experiments the half-widths of the  $c$  reflections are obviously broader than those of the  $a$  reflections. The line profile of the  $c$  reflections cannot be separated into sharp and diffuse contributions. They become very broad and quite anisotropic with rising temperature.

In Fig. 2 the corresponding results for the Miyake crystal are presented. Furthermore it is shown in Fig. 3(b) that the diffuse scattering connects, in a wavy-band pattern, lattice points that are separated by a  $[1\bar{1}0]$  reciprocal vector, similar to the diffuse scattering described in part I. Weissenberg photographs of the  $\mathbf{b}^*\mathbf{c}^*$  plane of the Miyake crystal are given in Fig. 3(a). Also in this plane the  $c$  line profiles are very diffuse and anisotropic along the  $\mathbf{b}^*$  direction. The photographs

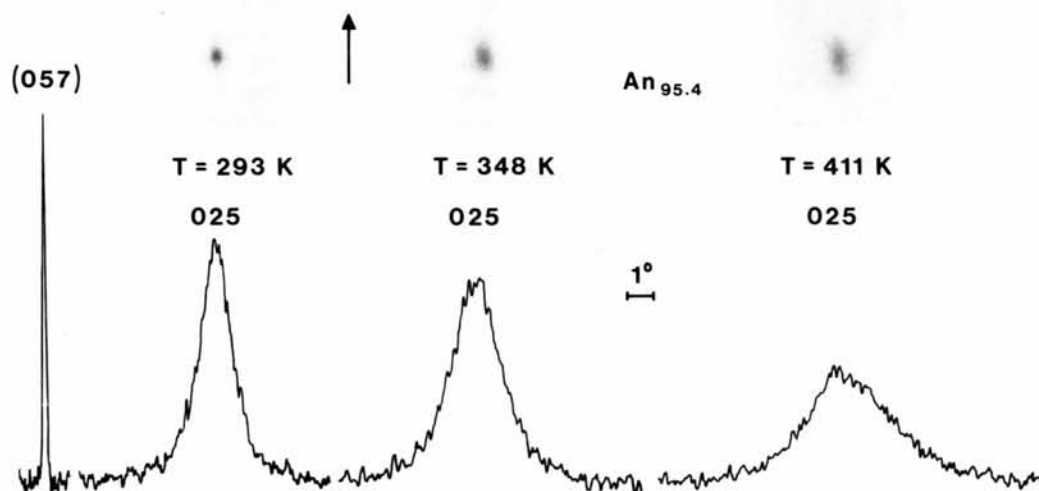


Fig. 2. Oscillation photographs and photometer curves as in Fig. 1 for  $\text{An}_{95.4}$ .

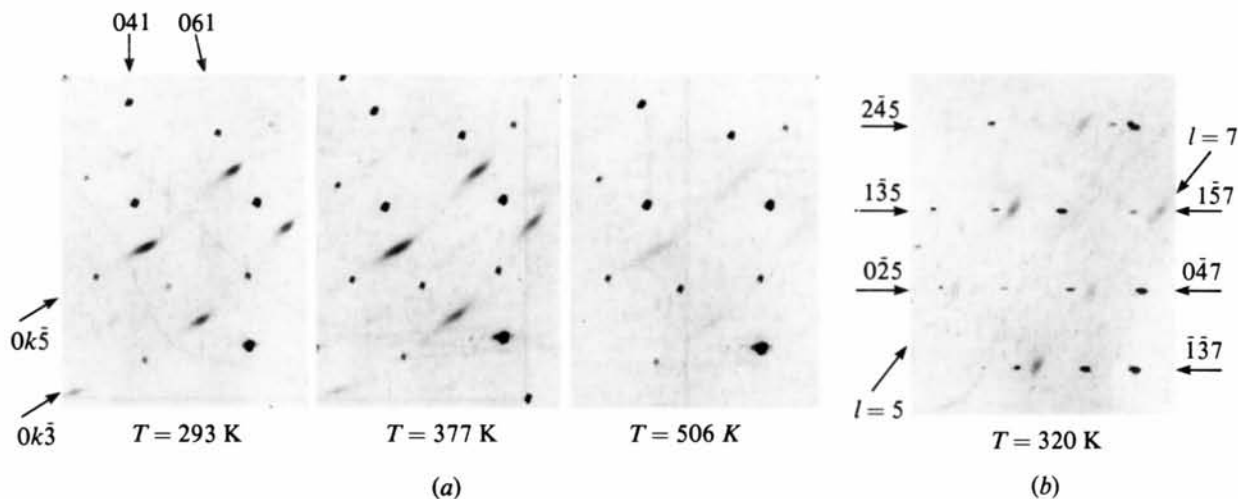


Fig. 3. Anisotropy of the diffuse scattering in  $\text{An}_{95.4}$ . (a) Magnified area of  $Ok\bar{l}$  Weissenberg photographs. (b) Section of a  $[100]$  oscillation photograph.

indicate a general broadening of the  $c$  and  $d$  reflections with rising temperature and a corresponding decrease of the intensities. At higher temperatures the diffuse scattering of the two investigated crystals has the same anisotropy as the diffuse contribution for  $An_{100}$  (Part I, Fig. 4).

The counter measurements were carried out as  $\omega$  scans across the 025 reflection. In the whole temperature range examined here, the fitting of a Lorentzian line gives much smaller standard deviations than that of a Gaussian line. The typical line profiles with

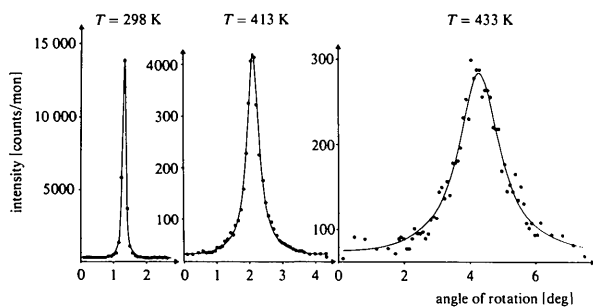


Fig. 4. Line profile of the 025 reflection of  $An_{97.5}$  recorded by counter technique ( $\omega$  scan). Intensity is given in counts per monitor (abbreviation: counts/mon). Lorentzian curves are fitted to the data.

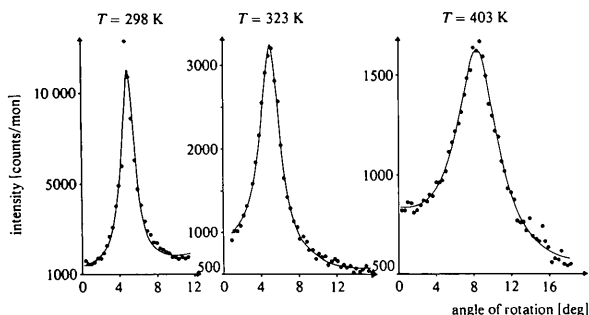


Fig. 5. Line profiles as in Fig. 4 for  $An_{95.4}$ .

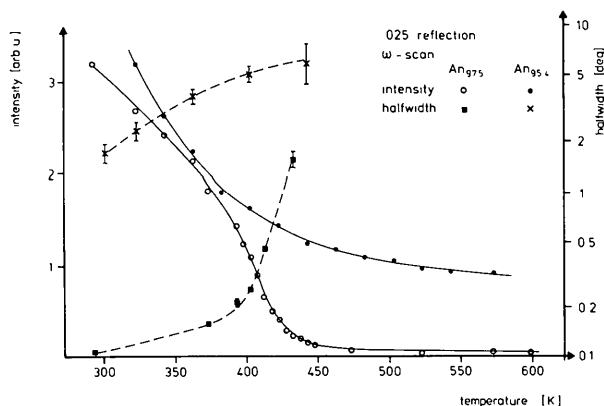


Fig. 6. Temperature dependence of the half-width and the peak intensity of the 025 reflection of  $An_{97.5}$  and  $An_{95.4}$  measured by counter technique ( $\omega$  scan).

fitted curves are shown in Figs. 4 and 5 for the samples of Mt. Somma and Miyake, respectively. In the latter case an asymmetric background contribution was used. Fig. 6 represents a graph of the peak intensities and the half-width of the line profiles as a function of temperature for the samples Mt. Somma and Miyake. A comparison between the half-widths taken from photometer curves of the two crystals is given in Fig. 7.

### (b) Neutrons

Only reflections of the [100] zone were measured: one  $a$  reflection: 004, two  $c$  reflections: 025 and 045, and one  $d$  reflection: 054. As expected, the two investigated samples show the same behaviour in every respect because of the almost identical chemical composition. The  $a$  reflection hardly depends on temperature; with rising temperature (up to 530 K) the intensity decreases only slightly. The half-width of 004 remains constant and amounts to  $17 \pm 1'$  for the purely elastic ones. Both values correspond to the resolution limit of the instrument. This is indicated by the fact that one Gaussian line can be fitted best to the measured profiles in accordance with the resolution theory.

The line profiles of the 045 reflection (Mt. Somma) are plotted in Fig. 8 for four different temperatures with integral as well as purely elastic measurements. For a better comparison Gaussian curves were fitted to the data. It is quite obvious that at about 510 K diffuse scattering at the place of the  $c$  reflection can only be detected for the integral measurement, whereas for the elastic setting the fitted Gaussian line does not represent a real intensity distribution anymore. It was assumed that the profiles are mainly determined by the resolution function of the instrument and therefore Gaussian lines were used. A direct comparison of the 045 reflection at 420 K demonstrates that a Lorentzian line yields a better fit; however, systematic deviations exist even here. Therefore a fit of two lines to the profiles gives the best results (Fig. 9). For our measurements it is impossible to decide whether this

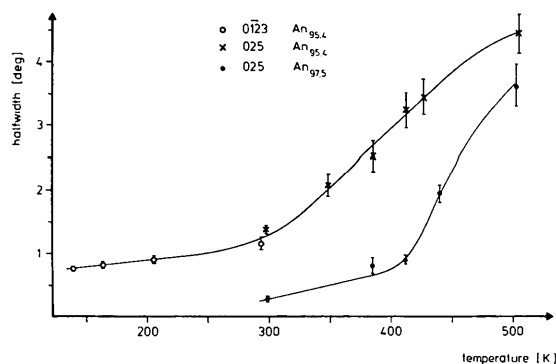


Fig. 7. Temperature dependence of the half-widths of  $c$  reflections. Comparison between  $An_{97.5}$  and  $An_{95.4}$ . Half-widths are taken from densitometer curves perpendicular to the layer line of oscillation photographs.

mixed character is caused by the folding of one Lorentzian line with a Gaussian line, which is determined by the resolution theory, or by two intensity contributions indicated by two different half-widths. In any case this problem cannot be solved above the phase

transition because low intensity makes it impossible to distinguish clearly between one Gaussian, one Lorentzian, or two Gaussian lines.

In Fig. 10 the half-widths of the 045 reflection are plotted as a function of temperature. Up to 390 K there is no difference between the half-widths of the integral and the elastic measurements. Yet above 420 K in both cases a broadening is obvious, being more distinct for the integral measurements. Above 490 K the reflection disperses for integral measurements, whereas it sharpens again for elastic measurements. Unfortunately, an analogous observation for the 025 reflection above  $T_c$  was prevented by the  $\lambda/2$  scattering of the 0,4,10 reflection. Fig. 11(a) shows the integral intensities of the 045 reflection (Mt. Somma) as a function of temperature registered with both measuring techniques. For the elastic measurements the intensity contribution disappears at about 530 K, whereas in the integral case

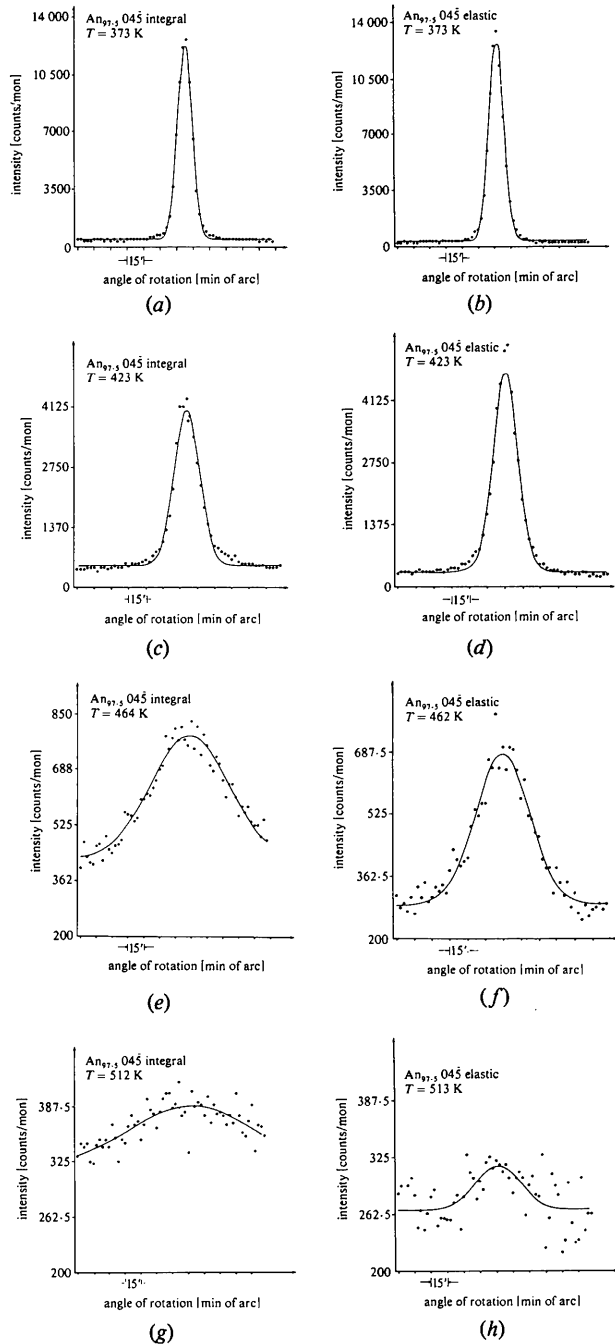


Fig. 8. (a)–(h) Integral and elastic measurements of the 045 reflection of  $An_{97.5}$  (sample: Mt. Somma,  $\omega$ -scan technique). Gaussian profiles are fitted to the data.

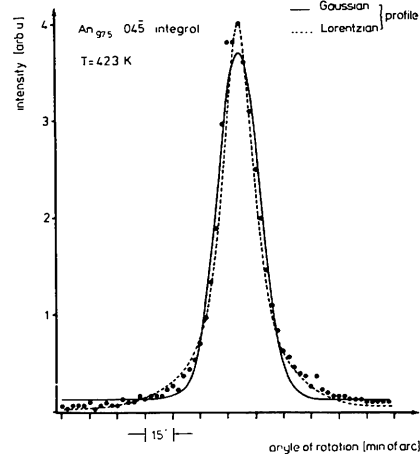


Fig. 9. Comparison of the Lorentzian and Gaussian fit to the line profile of the 045 reflection in  $An_{97.5}$  (Mt. Somma).

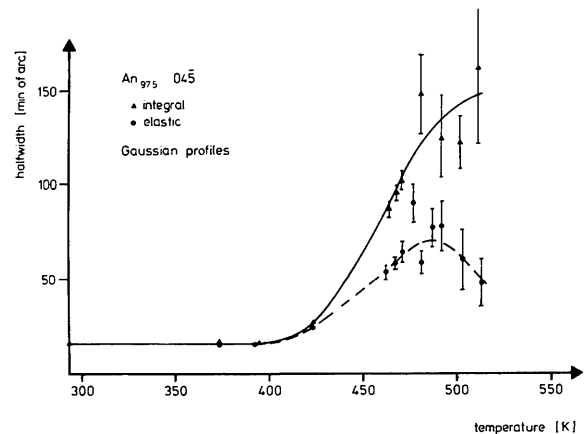
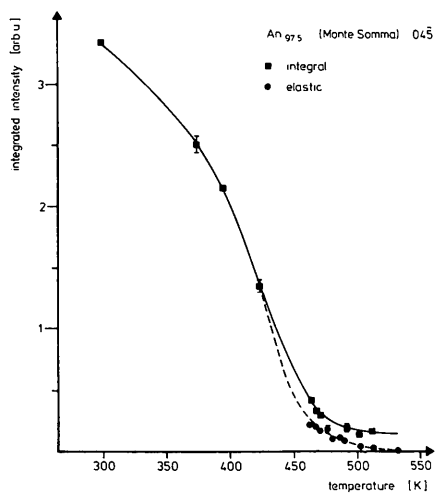
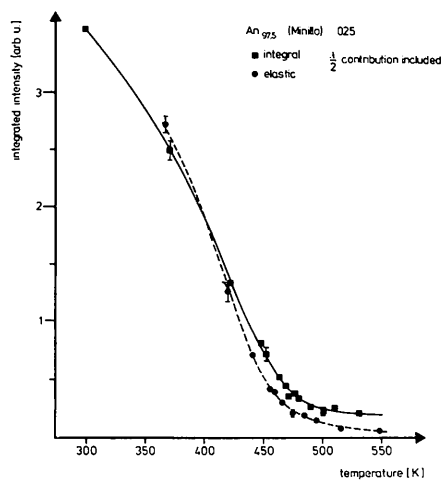


Fig. 10. Temperature dependence of the half-width of the 045 reflection in  $An_{97.5}$  (Mt. Somma). Comparison of integral and elastic measurements.



(a)



(b)

Fig. 11. (a) Integrated intensities of the  $04\bar{5}$  reflection of  $An_{97.5}$  (Mt. Somma) as a function of temperature. (b) Integrated intensities of the  $02\bar{5}$  reflection of  $An_{97.5}$  (Minillo) as a function of temperature.

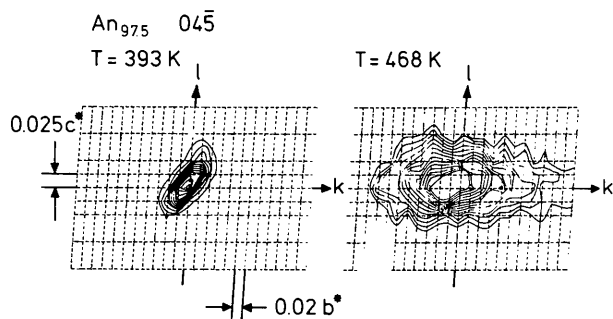


Fig. 12. Map of the diffuse intensity distribution around the  $04\bar{5}$  reflection in the  $(0kl)$  plane. ( $An_{97.5}$ , Mt. Somma, pure elastic measurements).

a distinct diffuse intensity is still detectable. All measured  $c$  reflections show the same behaviour as demonstrated in Fig. 11(b) by the  $02\bar{5}$  reflection of the Minillo crystal. In this case also the  $\lambda/2$  contamination causes a constant rest contribution.

Fig. 12 illustrates the distribution of the diffuse elastic intensity around the  $04\bar{5}$  reflection in the  $(0kl)$  plane for two different temperatures. The contour plot at 468 K is similar to the distribution of intensity noticeable in the Weissenberg photographs of  $An_{95.4}$  (Fig. 3a). At 468 K a half-width of about  $65'$  for an  $\omega$  scan of the  $04\bar{5}$  reflection can be deduced from Fig. 3(a). This corresponds to a value of  $0.16 |b^*|$ . A direct comparison with Fig. 12 demonstrates that this value matches completely the intensity distribution along the  $b^*$  axis.

### III. Discussion

The similarity of the temperature dependence of the sharp and diffuse scattering of  $c$  and  $d$  reflections found in both investigations (part I and this paper) enables us to use the common term 'c reflections' for the two types of reflections in the following discussion.

#### 1. Anorthite $An_{97.5}$ (Mt. Somma and Minillo)

With reduction in temperature, the same substantial change in the diffuse scattering at the  $c$  reflections was detected by X-ray as well as integral neutron measurements. As observed in  $An_{100}$  the diffuseness is anisotropic along the  $b^*$  and  $(a^* - b^*)$  directions. A comparison of the integral and purely elastic neutron measurements reveals the increasing contribution of the thermal diffuse scattering above 420–440 K, accompanied by a remarkable increase of the temperature gradient of the half-widths. This is probably caused by the growing influence of the TDS. Since the diffuse scattering intensity is completely beyond the energy window of the instrument at  $T \approx 530$  K, a temperature-dependent dispersion of the dynamical processes must be concluded. Above 530 K no more diffuse scattering of elastic or quasi-elastic origin can be observed. The model of Czank *et al.* (1973), therefore, proposing Ca atoms at  $P\bar{1}$  positions within an  $I\bar{1}$  matrix, is not compatible with this finding. As in  $An_{100}$  a reversible and complete phase transition exists but it is impossible to determine an exact critical point; the transition takes place over a temperature range. A comparison between the  $c$  intensities in  $An_{100}$  (part I) and  $An_{97.5}$  indicates that in  $An_{97.5}$  the range of the rapid decrease of intensity is shifted to lower temperatures for about 50 K. Particularly within this temperature range the profiles broaden and remain wide above  $T_c$ . For the elastic neutron measurements the behaviour is different (Fig. 10).

In contrast to  $An_{100}$  no separation between sharp and diffuse contributions within the transition range was possible. We suggest a superposition of two diffuse scattering contributions, thermal diffuse and antiphase domain scattering. But as for  $An_{100}$  the broadening of the half-widths is plausible because of the increasing TDS. It is most probable that an additional contribution is caused by fluctuations. However, with the experimental data at hand a clear separation of all different contributions cannot be performed.

For temperatures clearly below the transition range the striking difference between the integral and elastic measurements disappears. As described in § II, a careful line profile analysis of the  $c$  reflections measured by neutron diffraction below the phase transition has been carried out. It may be described best by two Gaussian lines, but we have no physical justification for this choice. However, in this case the X-ray results yield better information due to their higher resolution. The  $c$  profiles with a half-width of about  $6'$  are clearly broader than  $a$  and  $b$  reflections and can be fitted very well by Lorentzian lines (Fig. 4) in complete agreement with the photometer curves (Fig. 1). Summarizing, we may say that, disregarding the differing experimental resolutions, the X-ray and neutron measurements yield generally the same results for the low-temperature phase in  $An_{97.5}$ .

## 2. Anorthite $An_{95.4}$ (Miyake)

The X-ray measurements indicate principally the same behaviour of the diffuse scattering as observed in  $An_{97.5}$  above  $T = 420$  K. Again the anisotropy occurs along the  $\mathbf{b}^*$  direction (see Fig. 5). Compared to  $An_{100}$  the shape of the diffuse scattering is different, showing a 'structured' intensity distribution. With the photographs at hand we cannot decide whether these differences originate in static contributions causing diffuse profiles due to antiphase domains or in resolution effects. At lower temperatures the tendencies found for the transition  $An_{100} \rightarrow An_{97.5}$  are more pronounced: the transition range is enlarged further (*cf.* Foit & Peacor, 1973); a definite transition point cannot be discussed any more. In  $An_{97.5}$  a clear change of the temperature gradients of the half-widths occurs at around 400 K (Fig. 6). In  $An_{95.4}$  a similar change can be observed at room temperature (Fig. 7). If the crystal

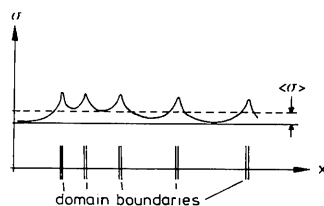


Fig. 13. Model for the stress distribution in an anorthite crystal with antiphase domain boundaries.

is cooled further to 138 K, the  $c$  reflections remain always wider than the  $a$  reflections, although their half-widths decrease continuously. As with  $An_{97.5}$  the line profiles are fitted best by Lorentzian lines (Fig. 5).

## IV. Soft-mode model

Several experimental findings, the occurrence of thermal diffuse scattering and its anisotropic distribution within the reciprocal space around the place of the  $c$  reflections, the broadening of the line profiles above the phase transition, and finally the direct proof of the inelastic origin of the scattering intensity indicates that the transition mechanism is initiated in principle as in pure anorthite. During the phase transition homogeneous fluctuations may also contribute to the scattering. But the absence of an exact transition point indicates new processes which are strongly coupled to the albite molecules. The question arises, which modification of the simple dynamical model based on the observations in pure anorthite is necessary for the new experimental results?

According to the electron microscopic results which indicate a domain structure, we may assume that the albite is mainly concentrated within the domain boundaries. With reference to the unit cell of anorthite all four subcells of albite are equal. Therefore, lattice distortions favouring an  $I\bar{1}$  structure will occur in the anorthite matrix. The distortions are distributed inhomogeneously, but no predictions about surrounding stress fields are possible. A simple schematic picture is drawn in Fig. 13 in order to explain the transition again with a dynamical model strongly suggested by the experiments. These new structural properties must be integrated into the theory.

Lattice distortions lead to a strain energy stored within the boundary and change at least the local potential conditions. If the additional stress,  $\sigma$ , is separated into an average contribution,  $\langle \sigma \rangle$ , and into local deviations,  $\Delta\sigma = \sigma - \langle \sigma \rangle$ , the influence of albite on the transition can easily be explained. Expanding the free energy in powers of the order parameter  $\eta$ , which we identify with the displacement of the atoms from their equilibrium positions in the  $I\bar{1}$  phase, a contribution  $\langle \sigma \rangle \eta$  to the atomic potential is added, taking into account the stress  $\langle \sigma \rangle$ . Therefore, we can write

$$F = (a + a')\eta^2 + b\eta^4 + \dots,$$

with the constant  $a' = \langle \sigma \rangle / \eta > 0$  and  $b > 0$ , neglecting terms of higher order in  $\eta$ .  $a$  is the well-known coefficient in Landau's expansion with a temperature dependence of

$$a > 0 \text{ for } T > T_c,$$

$$a = 0 \text{ for } T = T_c,$$

$$a < 0 \text{ for } T < T_c.$$

and

$T_c$  is the transition temperature for pure anorthite  $An_{100}$ . Now, the phase transition does not occur when  $a(T = T_c) = 0$ , but at  $T_0 < T_c$ , when the condition  $a(T_0) + a' = 0$  is fulfilled. Thus the transition temperature is shifted to lower temperatures.

The introduction of a homogeneous stress,  $\langle\sigma\rangle$ , leads to a change of the free energy and consequently to a new average structure. Because  $\langle\sigma\rangle$  favours the  $I\bar{1}$  structure the intensity of the  $c$  reflection is decreased, whereas the intensities of the  $a$  and  $b$  reflections remain nearly unchanged. Moreover, the striking temperature dependence of the intensity of the  $c$  reflection at room temperature in  $An_{97.5}$  and even more in  $An_{95.4}$  can easily be explained by the reduction of the transition temperature. Since the stresses vary locally, depending on the fluctuations,  $\Delta\sigma$ , a large range of values for  $a'$  and consequently for  $T_0$  exists. Within the crystal volume the transition is now spread out over a finite range. But it is still a continuous transition. Nevertheless, it is plausible that large fluctuations in  $\sigma$  cause considerable anharmonic-potential contributions which are taken into account by a further cubic term in the expansion of  $F$ :

$$F = (a + a')\eta^2 - c\eta^3 + b\eta^4. \quad (1)$$

This leads to a complete change of the character of the transition. As a result we find a transition of first order and, in consequence, hysteresis effects and the possibility of heterogeneous fluctuations. These fluctuations may exist far from the transition temperature, thus contributing to a further widening of the transition range. Because of the asymmetry of  $F$  with respect to  $\eta$  only one absolute minimum develops in the low-temperature phase; therefore only one of the two antiphase positions will be realized or at least preferred. Complicated mixed behaviour of the transition can now result from the local character of the constant  $c$ . But beyond the transition range it will be basically the same as in  $An_{100}$ . In particular, the influence of a cubic term can only be observed for large displacements produced by a soft mode and at the phase transition where the contribution  $(a + a')\eta^2$  is small.

### V. Transitional anorthite

The phenomenological soft-mode model used for the discussion of the phase transition provides a good description of  $An_{100}$  and explains also the diffuse scattering and the temperature dependence of  $An_{97.5}$  and  $An_{95.4}$ . But we know from the preceding discussion that the gradual insertion of albite molecules changes the behaviour at the phase transition drastically. The character of a real phase transition is lost more and more and this can be explained by a static disorder of the anorthite structure. Although the X-ray results may still be explained by the proposed

dynamical model, the increase of the transition range as well as the lowering of the transition temperature indicate a growing influence of a static disorder correlated with the Ab molecules. Thus, complete transition by a dynamic process will be suppressed.

In a completely different approach we may consider the influence of albite coming from plagioclases with high Ab content, *i.e.* bytownites or labradorites, and try to extend these considerations to the transitional anorthite under investigation. As discussed elsewhere (Jagodzinski & Korekawa, 1976) there are some structural invariants common to all plagioclases within the concentration range  $0.5 \leq x \leq 1$ . In particular there are chains in the [001] direction which are defined by the shortest cation distances. Let us denote the chain through the origin by the symbol  $A$  and the chains through the  $(\frac{1}{2}, \frac{1}{2}, 0)$  and  $(\frac{1}{2}, \frac{1}{2}, 0)$  positions, which are topochemically equal and topologically slightly different, by the symbol  $B$ . An interruption in the sequence  $\dots ABAB \dots$ , *e.g.*  $ABAABAB \dots$ , leads to an antiphase boundary with a fault vector  $[\frac{1}{2}, \frac{1}{2}, \frac{1}{2}]$ . This interruption can be caused by small atomic displacements as described by the model of Czank *et al.* (1973). Consequently, the problem of antiphase domains may at least formally be described by two-dimensional statistics of chains. If we introduce the terms  $\Delta E_1$  for the difference in interaction energies\* between an  $AA$  (or  $BB$ ) and an  $AB$  sequence in the [110] direction and  $\Delta E_2$  for the analogous difference in the  $[1\bar{1}0]$  direction, the whole problem can be described by a modified two-dimensional Ising model. As shown by Onsager (1944), the critical temperature,  $T_c$ , for the order-disorder transition of this system is given by

$$\sinh(\Delta E_1/kT_c) \sinh(\Delta E_2/kT_c) = 1.$$

Obviously, a decrease of  $\Delta E_1$  and/or  $\Delta E_2$  leads to a lowering of the critical temperature  $T_c$ . As discussed in § IV, an averaged strain of the lattice due to Ab boundaries will lead to such a decrease in  $\Delta E_1$  and/or  $\Delta E_2$ . By the Ab boundaries the crystal will be divided into small, nearly independent domains and, according to Onsager (1944), critical behaviour no longer exists for such a finite system. Consequently, the broadening of the transition range with increasing Ab content may also be explained in this way. A shift of the maximum of the pseudo-critical fluctuations to lower temperatures is also indicated, but it remains uncertain whether this change is sufficiently large to explain the considerable change observed in our samples. On the other hand, a *quantitative* application of this crude model to our experiments seems to be irrelevant. Therefore, it should be pointed out that no decision can be made whether this finite volume effect or the strain fluctuations discussed in § IV have the main influence on the observed changes in the transition range.

\* The  $\Delta E_i$  represent free energies rather than static potentials in this case.



## VI. Antiphase domains

A discussion of the behaviour of the antiphase domains must be limited to the temperature range  $T \leq 420$ – $450$  K and  $T$  lower than room temperature for  $An_{97.5}$  and  $An_{95.4}$ , respectively; only here is the thermal diffuse scattering contribution comparatively small (see § III.1).

Electron microscope bright- and dark-field images indicate the existence of  $c$  domains with sizes between 200 and 2000 Å. Their average size must be smaller than 2000 Å, since not all antiphase domain boundaries show a sensitive contrast when the dark-field technique is used (Müller, Wenk & Thomas, 1972). The size of the domains remains constant, even after heating the crystals to about 800 K and cooling down again (shape-memory effect). By the high-resolution X-ray methods we can estimate from the reflection widths an average domain size of about 1700 Å in  $An_{97.5}$  at room temperature. The reflection widths become considerably broader with rising temperature, apparently in contradiction to EM findings. One possible explanation is based on an interaction between adjacent domains, preferring an equal-phase state for neighbouring domains. It is unimportant whether a reference domain is in the 'in-phase' (+) or 'out-of-phase' (–) state. The mutual influence across the domain boundaries cannot be a purely static phenomenon since X-ray and neutron measurements should supply temperature-independent line widths. If the process is time dependent the domains must fluctuate between the '+' and '–' phases, and their average state in one phase can be described by a characteristic lifetime,  $t$ . This assumption fits well to the antiphase model of Czank *et al.* (1973) mentioned in § I. To change from a '+' state to a '–' state the atoms must only move over a small distance. The two possible positions per atom correspond exactly to the potential minima allowed for the  $P$  phase in the Landau theory for continuous phase transitions. Here the asymmetry of the two minima caused by the  $c\eta^3$  contribution in (1) is neglected. Furthermore, the time dependence of the interaction must be described by an average relaxation time  $\tau$ , indicating the time a neighbouring domain needs to change into the state of the reference domain. If the interaction prefers the same state as the neighbouring domains, the domain structure is effectively coarsened and consequently the quasi-elastic scattering sharpened. As will be discussed in a further publication, the reflection is proportional to  $\tau/t$ . Hence, the change of line widths with constant domain sizes can be explained with varying characteristic times  $t$  and  $\tau$ . Another explanation for the behaviour of the domains may be given again by the Ising model discussed in § V.  $\Delta E'_1$  and  $\Delta E'_2$  describe now the difference in the average interaction energies between adjacent domains being in the same or in a different phase state. This model can

explain the varying line widths by a change of the correlation length of equal-phase states for different domains. Also in this model an order–disorder transition may occur at a new critical temperature  $T'_c$ . At this temperature all domains change into the same phase state, leading to a sudden narrowing of the  $c$  reflections.

However, the coarsening introduced in both models explains quite naturally the existence of smaller domains in connection with sharp  $c$  reflections as observed by electron microscopic photographs. But again, this coarsening effect prevents the determination of an average domain size by conventional X-ray or neutron measurements.

## VII. Conclusions

For all three investigated samples the  $c$  and  $d$  reflections behave the same. Both X-ray and neutron measurements at temperatures ranging between 140 and 570 K show that these reflections are obviously broader compared with the  $a$  and  $b$  reflections. The half-widths of the  $c$  reflections depend considerably on temperature. This dependence is most striking within the transition range. The behaviour of intensity and anisotropy of the diffuse scattering contribution is basically the same as in  $An_{100}$ ; therefore we suggest the same reasons for the phase transition. It was found with neutrons that the diffuse scattering is of inelastic origin. Furthermore, the observed temperature dependence of the dispersion agrees completely with the model assuming a softening of the dynamical wave. Even small albite concentrations have a considerable influence on the behaviour at the transition from a primitive to a body-centered arrangement. Although the transition is still reversible and complete—this observation is contradictory to models based on purely static interpretations of all diffuse scattering contributions—the transition is spread over a certain temperature range and shifted to much lower temperatures. In  $An_{95.4}$  the transition is already in progress at room temperature, hence, it is very difficult to separate experimentally the contributions of thermal diffuse scattering and of antiphase domain scattering. Therefore, we want to emphasize that interpretations of conventional diffractometer data with respect to structural refinements at this temperature could be erroneous. As in  $An_{100}$  the model of the phase transition yields the formation of antiphase domains in the low-temperature phase. In addition, explanations for the varying half-widths of the  $c$  reflections at constant domain size are given. The soft-mode model allows for two equal atomic positions with the  $P\bar{1}$  phase, corresponding to an 'in-phase' and an 'antiphase' condition. The domains can fluctuate between both positions. Interactions across the domain boundaries

lead to virtually coherent areas of domains with the same phase state. Thus the line width is a function of the statistics of the domain configurations and the strength of the interaction which depends on temperature and the characteristics of the domain boundary.

We wish to acknowledge the financial support by the Deutsche Forschungsgemeinschaft (project Ja 15/32).

#### References

- ADLHART, W., FREY, F. & JAGODZINSKI, H. (1980). *Acta Cryst.* **A36**, 450–460.  
 BROWN, W. L., HOFFMANN, W. & LAVES, F. (1963). *Naturwissenschaften*, **50**, 221.  
 CZANK, J., VAN LANDUYT, J., SCHULZ, H., LAVES, F. & AMELINCKX, S. (1973). *Z. Kristallogr.* **138**, 403–418.  
 FOIT, F. F. JR & PEACOR, D. R. (1973). *Am. Mineral.* **58**, 665–675.

- HEUER, A. H. & NORD, G. L. JR (1976). *Polymorphic Phase Transitions in Minerals*. In *Electron Microscopy*, edited by H. R. WENK, Chapter 5.1. Berlin: Springer.  
 HEUER, A. H., NORD, G. L. JR, LALLY, J. S. & CHRISTIE, J. M. (1976). *Origin of the (c) Domains in Anorthite*. In *Electron Microscopy*, edited by H. R. WENK, Chapter 5.7. Berlin: Springer.  
 JAGODZINSKI, H. & KOREKAWA, M. (1973). *Geochim. Cosmochim. Acta*, Suppl. 4, Vol. 1, 933–951.  
 JAGODZINSKI, H. & KOREKAWA, M. (1976). *Z. Kristallogr.* **143**, 239–277.  
 LAVES, F., CZANK, M. & SCHULZ, H. (1970). *Schweiz. Mineral. Petrogr. Mitt.* **50**, 519–525.  
 MCLAREN, A. C. & MARSHALL, D. B. (1974). *Contrib. Mineral. Petrol.* **44**, 237–249.  
 MÜLLER, W. F., WENK, H. R., BELL, W. L. & THOMAS, G. (1973). *Contrib. Mineral. Petrol.* **40**, 63–74.  
 MÜLLER, W. F., WENK, H. R. & THOMAS, G. (1972). *Contrib. Mineral. Petrol.* **34**, 304–314.  
 ONSAGER, L. (1944). *Phys. Rev.* **65**, 117–149.

*Acta Cryst.* (1980). **A36**, 470–475

## The Use of Higher Invariants in *MULTAN*

BY A. A. FREER AND C. J. GILMORE

*Department of Chemistry, University of Glasgow, Glasgow G12 8QQ, Scotland*

(Received 20 August 1979; accepted 24 December 1979)

#### Abstract

A method of using quartets and quintets in the direct-methods program *MULTAN* is described with several successful applications.

#### Introduction

*MULTAN* is the most widely used direct-methods computer program. Several extensions to the system have been described recently in which magic integer/ $\psi$  map and random phase set/linear equation algorithms have been employed (Declercq, Germain & Woolfson, 1979). These developments undoubtedly enhance the power of the program. However, they are confined to the use of three-phase invariants. Recently, there has been considerable activity in deriving formulae for estimating the magnitudes of four- and five- phase structure invariants (Hauptman, 1977*a,b*; Giacovazzo, 1976*a,b*; van der Putten & Schenk, 1977). These relationships contain new phase information, and it is therefore a logical extension of the *MULTAN* procedure

to incorporate them into this program and determine any advantages that thereby accrue.

Two modes of usage of higher invariants must be distinguished:

- (a) the active mode in which the invariants are used to generate new phase information;
- (b) the passive mode where the invariants are used only for figures of merit for selecting the most probable phase set.

Of course, the use of (a) does not preclude the use of (b) and both techniques will be discussed in this paper.

#### Quartets

The *MULTAN* 78 program was modified to use the seven-magnitude, second neighbourhood  $P_{1/7}$  and the 13-magnitude, third neighbourhood  $P_{1/13}$  joint conditional probability distributions of Hauptman (1977*a*) for the non-centrosymmetric case and the corresponding  $P_7^\pm$  and  $P_{13}^\pm$  formulae for centrosymmetric space groups (Hauptman, 1977*b*). These formulae give reliable invariant estimates for all combinations of the